Chaotic behavior of the Fermi–Pasta–Ulam β–model with different ranges of particle interactions

Helen Christodoulidi[1], Tassos Bountis[1], Constantino Tsallis[2,3] and Lambros Drossos[4]
[1]Department of Mathematics, Division of Applied Analysis and
Center for Research and Applications of Nonlinear Systems (CRANS),
University of Patras, GR-26500 Patras, Greece.
[2]Centro Brasileiro de Pesquisas Fisicas and
National Institute of Science and Technology for Complex Systems,
Rua Xavier Sigaud 150, 22290-180 Rio de Janeiro-RJ, Brazil
[3]Santa Fe Institute, 1399 Hyde Park Road, Santa Fe, NM 87501, USA
[4]High Performance Computing Systems and Distance Learning Lab (HPCS-DL Lab),
Technological Educational Institute of Western Greece,
GR-26334 Patras, Greece

May 30, 2016

Abstract

In the present work we study the Fermi–Pasta–Ulam (FPU) β–model involving long range interactions (LRI) in both the quadratic and quartic potentials, by introducing two independent exponents α_1 and α_2 respectively, which make the system's forces decay with distance r. Our results demonstrate that weak chaos, in the sense of decreasing Lyapunov exponents and q–Gaussian probability density functions (pdfs) of sums of the momenta, occurs only when long range interactions are included in the quartic part. More importantly, for $0 \leq \alpha_2 < 1$, we obtain extrapolated values for $q > 1$, as $N \to \infty$, suggesting that these pdfs persist in that limit. On the other hand, when long range interactions are imposed only on the quadratic part, strong chaos and purely Gaussian pdfs are always obtained.

1 Introduction

In recent years, many authors have examined the effect of long range interactions on the dynamics of multi–dimensional Hamiltonian systems [1, 2, 3, 4, 5, 6, 7, 8]. It has thus been found that a number of these systems show a more organized behavior, as exemplified by a decreasing maximal Lyapunov exponent (MLE) over long integration times. Perhaps the best known example in this class is the so–called Hamiltonian Mean Field model, where the MLE was shown numerically to decrease with increasing number of degrees of freedom N, according to a specific power law [2, 3, 6, 7]. More recently, another famous example in this category, the FPU β–Hamiltonian was studied in the presence of long range interactions. In the complete absence of harmonic terms the MLE appears to vanish in the thermodynamic limit [9, 10]. Moreover, when harmonic terms are included in the potential, a similar behavior of the MLE is observed [11], which nevertheless tends to saturate to a non–zero value above a characteristic size N.

It is the purpose of the present paper to investigate more thoroughly the FPU β–model from this point of view, by studying the effect of the interactions through two parameters α_1 and α_2 introduced in the quadratic and quartic terms of the potential respectively. In so doing, we will be able to identify domains of

strong and weak chaos, by examining whether probability density functions (pdfs) of sums of the momenta obey Boltzmann Gibbs (BG) statistics or not.

The maximal Lyapunov exponent and other indicators of local dynamics [12] provide useful tools for chaos detection, but are not well suited for distinguishing between different degrees of weak vs. strong chaos [13]. For example, if a given orbit is chaotic, its MLE is expected to converge to a positive value. However, if the orbit is trapped for a long time near islands of regular motion, the MLE does not quickly converge and when it does, one cannot tell from its value whether the dynamics can be described as weakly or strongly chaotic.

Now, long range systems are known to possess long living quasi–stationary states (QSS) [14, 15, 16, 17, 18, 19, 20, 21, 22, 23, 24, 25, 26, 27], whose statistical properties are very different from what is expected within the framework of classical BG thermostatistics [28]. More specifically, when one studies such QSS in the spirit of the central limit theorem, one finds that the pdfs of sums of their variables are well approximated by q–Gaussian functions (with $1 < q < 3$) or q–statistics [29, 30, 31, 32, 33]. These pdfs last for very long times beyond which they are expected to tend to the $q = 1$ case of pure Gaussians and BG thermal equilibrium. Thus, we will treat the index q as a measure of the "distance" from a Gaussian, and study its time evolution to identify when a "phase transition" will occur from weak chaos and $q > 1$–statistics to strong chaos and BG thermostatistics.

In this context, it becomes highly relevant to examine the effect of the range of the interactions on the lifetime of a QSS, and hence the duration of weakly chaotic dynamics. To this end, we recently introduced and studied numerically a generalization of the FPU β–model, in which we varied the interaction range by multiplying the quartic terms of the potential by coupling constants that decay with distance as $r^{-\alpha}$ [11]. The pdfs of the time–averaged momenta were thus found to be well approximated by q–Gaussians with $q > 1$, when the range is long enough (i.e. $\alpha < 1$). This, however, lasts up to a crossover time $t = t_c$ at which q starts to decrease monotonically to 1, reflecting the transition from q–statistics to BG thermostatistics.

In the present paper, we extend our study and investigate additional properties connected with the occurrence of weakly chaotic QSS, taking a closer look at their dynamics as well as associated statistics. In particular, we consider the FPU β–chain [34] of N particles, whose potential includes harmonic as well as quartic interactions, and employ two different exponents α_1 and α_2, for the $r^{-\alpha}$ coupling constants of the quadratic and quartic terms respectively. Furthermore, we vary these exponents independently to investigate their effect on the thermostatistics of the orbits at increasingly long times. A recent study on long range interactions applied only on the harmonic terms can be found in [35].

In Section 2, we write the Hamiltonian of our model as the sum of its kinetic and potential energies and explain the two exponents that determine the range of the interactions. Next, in Section 3, we present a detailed study on the behavior of the maximal Lyapunov exponents when long range is applied either to the quadratic (linear LRI) or the quartic (nonlinear LRI) part of the potential. We choose random initial conditions and compare the dynamics and statistics of these cases computing the pdfs of the sums of their momenta for sufficiently long times.

In Section 4, we examine the value of q, and other parameters on which the pdf depends, focusing especially on the thermodynamic limit, where the total energy E and N tend to infinity at fixed specific energies $\varepsilon = E/N$. We thus discover, for $0 \leq \alpha_2 < 1$, a *linear* relation between q and $1/\log N$, which allows us to extrapolate the value of $q = q_\infty$ in the limit $N \to \infty$. Since we thus end up with values $q_\infty > 1$, we conclude that q–Gaussian pdfs behave as if they were *attractors* and hence that q–statistics prevails over BG thermostatistics in that limit. Finally in Section 5 we present our conclusions.

2 The FPU β–model with different ranges of interaction

Let us consider the famous Fermi–Pasta–Ulam β–model of a 1–dimensional lattice of N nonlinearly coupled oscillators governed by the Hamiltonian

$$\mathcal{H}_{FPU} = \frac{1}{2}\sum_{n=1}^{N} p_n^2 + \sum_{n=0}^{N} V_2(x_{n+1} - x_n) + \sum_{n=0}^{N} V_4(x_{n+1} - x_n) \quad , \tag{1}$$

involving nearest–neighbor interactions, where V_2 and V_4 represent the quadratic and quartic functions $V_2(u) = au^2/2$ and $V_4(u) = bu^4/4$. The p_n, x_n are the canonical conjugate pairs of momentum and position variables assigned to the nth particle, with $n = 1, 2, ..., N$ and fixed boundary conditions, i.e. $x_0 = x_{N+1} = p_0 = p_{N+1} = 0$.

In this paper we modify the above classical form of the FPU β–model by introducing the parameters α_1 and α_2, which enter in the linear and nonlinear parts of the equations of motion, to determine the particle interactions that decay with distance as $1/r^{\alpha_1}$ and $1/r^{\alpha_2}$ respectively. In particular, the modified Hamiltonian function that describes the generalized FPU β–system has the form

$$\begin{aligned} \mathcal{H}_{LRI} = \quad & \frac{1}{2}\sum_{n=1}^{N} p_n^2 + \frac{a}{2\widetilde{N}_1}\sum_{n=0}^{N}\sum_{m=n+1}^{N+1}\frac{(x_n - x_m)^2}{(m-n)^{\alpha_1}} \\ & + \frac{b}{4\widetilde{N}_2}\sum_{n=0}^{N}\sum_{m=n+1}^{N+1}\frac{(x_n - x_m)^4}{(m-n)^{\alpha_2}} \quad , \end{aligned} \tag{2}$$

where a and b are positive constants.

Note that there are three ways to introduce long range interactions (LRI) in our model: (a) only in the quadratic potential V_2, (b) only in the quartic potential V_4 and (c) both in V_2 and V_4. Case (b) was the one studied in [11] and gave the results mentioned above, where a "phase transition" occurs between q–statistics and BG thermostatistics near the value $\alpha_2 = 1$ that separates the short term $\alpha_2 > 1$ from the long term $0 \leq \alpha_2 < 1$ interaction range.

As explained above, the critical value $\alpha_1 = \alpha_2 = 1$ is expected to determine the crossover between long and short range interactions. When $\alpha_i < 1$, $i = 1, 2$ the interactions are long range, with the lower bound $\alpha_i = 0$ signifying that each particle interacts equally with all others, exactly as in a fully connected network. In contrast, when $\alpha_i > 1$, $i = 1, 2$, the interactions are short range and in the limit $\alpha_i \to \infty$ only the nearest neighbor terms survive in the sums and the classical form of the FPU β–Hamiltonian is recovered.

The rescaling factors $\widetilde{N}_i$, $i = 1, 2$ in (2) are given by the expression

$$\widetilde{N}_i(N, \alpha_i) \equiv \frac{1}{N}\sum_{n=0}^{N}\sum_{m=n+1}^{N+1}\frac{1}{(m-n)^{\alpha_i}}, \quad (i = 1, 2) \tag{3}$$

and are necessary for making the Hamiltonian extensive. Indeed, without this factor the sums of V_2 and V_4 in (2) would increase as $(N + 1)(N + 2)/2$ in the thermodynamic limit, thus rendering the kinetic energy (which grows like N) irrelevant [11]. Notice that $\widetilde{N}_i \simeq 1$ in the limit $\alpha_i \to \infty$, and thus for large N Hamiltonian (2) reduces to Hamiltonian (1).

3 Conditions for weak chaos and q–thermostatistics

3.1 Linear versus non-linear long range interactions

It has been known for some time (see e.g. [2, 3]) that Hamiltonian systems possessing LRI display a more organized behavior in the thermodynamic limit. It is also well established that the maximal Lyapunov exponent λ of the FPU β–system converges to a positive constant in the thermodynamic limit, that depends only on the coupling constant b and on the system's specific energy ε. What happens, however, when linear and/or non-linear interactions between distant particles are taken into account? Choosing to work on the FPU β–model in the present paper, provides the advantage of making a direct comparison between linear and non-linear LRI and allows us to examine in detail their effect on the system's dynamics.

Note that system (2) can be studied in the presence of only linear LRI by taking $\alpha_2 \to \infty$ and letting α_1 act as a free parameter that controls the range of interaction. This means that the potential V_4 in that case is equivalent to the one used in the classical FPU β–model. By contrast, if we wish to study the effect of nonlinear LRI alone, we take $\alpha_1 \to \infty$ and α_2 becomes the free parameter.

Let us now display in Fig.1 the behavior of the maximal Lyapunov exponent $MLE = \lambda$, in the above cases, first in terms of the system size N and then as a function of the specific energy ε ($a = 1$ in every case). Panels (a) and (b) are for $b = 1$, $\varepsilon = 1$ and $b = 10$, $\varepsilon = 9$ respectively. Both of them include values λ_{FPU} of the classical FPU β–model as a point of reference, which separate the two LRI cases: Under λ_{FPU} we find the maximal Lyapunov exponents λ_{V4} of the nonlinear LRI case, while above we encounter the λ_{V2} exponents. Note that the longer the range of interaction, the higher the λ_{V2} values. For $\alpha_1 = \alpha_2 = 10$ the λ_{V2} and λ_{V4} curves collapse to the λ_{FPU} values.

In Fig.1(a) the MLEs λ_{V2} and λ_{V4} grow very slowly and even tend to tend to saturate as $N \to \infty$. By contrast, in Fig.1(b,) for $\varepsilon = 9$ and $b = 10$, this tendency is reversed in the case of the λ_{V4} exponents which are seen to decrease with N. The reason this is not observed in Fig.1(a) is because it requires high $b\varepsilon$ values, as pointed out already in [11]. An additional remark is that, for $\alpha_2 = 0$ the exponents λ_{V4} of Fig.1(b) seem not to vanish for $N \to \infty$, but tend to saturate at a positive value. Only when the quadratic part V_2 ($a = 0$ in (2)) is completely eliminated from the Hamiltonian, the Lyapunov exponents continue to fall to zero as N keeps increasing (see [9] for a detailed numerical study of this issue and [10] for a theoretical justification in the limit $N \to \infty$).

So, what are the $b\varepsilon$ values that yield a power–law decrease of λ_{V4} vs. ε? When is the system weakly chaotic and why? To find out we have computed the MLEs at various specific energies, keeping the parameter $b = 1$ fixed and the number of particles $N = 8192$. As Fig.1(c) clearly shows, linear LRI (represented by the upper curve of squares) make the system much more chaotic than the classical nearest neighbor FPU case (represented by the middle curve of circles). We believe that this is due to the fact that the implementation of LRI on the linear part of the Hamiltonian results in a "compression" of the phonon band $\omega_k = 2\sin\frac{k\pi}{2(N+1)}$ of the nearest neighbor case ($\alpha_1 = \infty$) from the interval $[0, 2]$ to a single point with frequency $\Omega = \sqrt{2(N+2)/(N+1)}$, as α_1 tends to zero. This suggests that no sizeable region of quasiperiodic tori exists to sustain regular motion, while the periodic oscillations of the lattice (with frequency Ω) that become unstable due to the presence of nonlinear terms should have large scale chaotic regions regions about them that dominate the dynamics in phase space.

On the other hand, when LRI apply only to the nonlinear part of the Hamiltonian and the harmonic terms are of the nearest neighbor type it is interesting to compare the chaotic behavior of the system with that of the classical FPU model. As Fig.1(c) clearly demonstrates, the corresponding MLE curves are very close to each other when ε is small, but begin to deviate considerably for $\varepsilon > 1$. Indeed, the application of nonlinear LRI is characterized by much weaker chaos in the limit $\varepsilon \to \infty$ as its MLE behaves like $\lambda_{V4} \sim \varepsilon^{0.05}$, in contrast with the FPU model whose corresponding MLE grows a lot faster, as $\lambda_{FPU} \sim \varepsilon^{1/4}$ (see [36] for an analytical derivation). It is also interesting to note that in this limit the exponents λ_{V2}

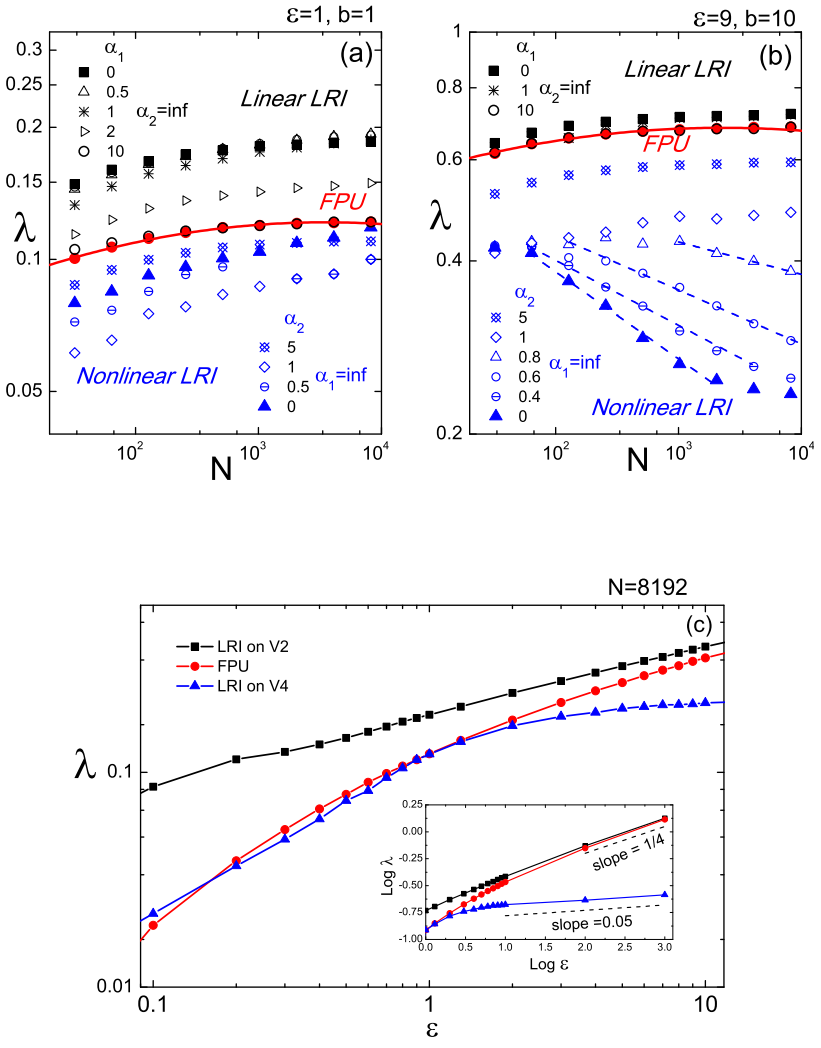

Figure 1: Log–log plots of MLE values at $t = 10^6$: (a) For increasing N, with $b = 1$ and $\varepsilon = 1$, (b) as N increases with $b = 10$ and $\varepsilon = 9$ and (c) as a function of ε at $N = 8192$, $b = 1$, for 3 cases: An upper curve of black squares for LRI on V_2 only with $(\alpha_1, \alpha_2) = (0, \infty)$, the middle one of red circles for the classical FPU case with $(\alpha_1, \alpha_2) = (\infty, \infty)$ and a lower one of blue triangles for LRI on V_4 only for $(\alpha_1, \alpha_2) = (\infty, 0)$.

and λ_{FPU} become indistinguishable.

Remarkably, the above picture of the maximal Lyapunov exponent λ_{V4} slowing down as the specific energy grows is accompanied by the emergence of q–Gaussian distributions in the momenta associated with the presence of weakly chaotic behavior. In the next subsection we examine this phenomenon more carefully as we concentrate our study on the statistical aspects of the LRI models.

3.2 Emergence of q–Gaussian distributions

Besides this striking difference of the level of chaoticity in the above two (short and long range) situations, there is also a remarkable difference in their statistics, as we are going to explain.

The pdfs we shall study correspond to orbits specified by the momentum vectors $\mathbf{p} = (p_1, \ldots, p_N)$ evaluated at discrete times starting from a uniform distribution. In particular, these time averaged pdfs are calculated from the collection of data at $t > t_0$, where the kinetic energy has stabilized and at multiples of a time interval τ large enough to avoid correlations. We then assign to the i–th band of our histograms the number of times that the momenta $p_i(k\tau)$, $i = 1, \ldots, N$ fall in that band and rescale.

In the four panels of Fig. 2 typical momentum histograms are shown, which correspond to the application of different interaction ranges contained separately in V_2 and V_4. More specifically, in panels (a) and (c) a classical Gaussian shape is observed, either under purely short range interactions or when LRI apply only to the quadratic part by setting $a_1 = 0.7$ and $a_2 \to \infty$ in the Hamiltonian (2). In panels (b) and (d) a clear q–Gaussian shape emerges when long range applies to the quartic interactions, independently of interactions in the quadratic part, i.e. for $a_1 \to \infty$, $a_2 = 0.7$ and $a_1 = 0.7$, $a_2 = 0.7$ in (2) respectively.

In practice, we have employed an algorithm which uses the least squares method to calculate q, determines the intercept and estimates β from the slope of the resulting straight line. Dividing then the q interval [1,3] into 1000 possible values, we apply the least squares method to all of them. The appropriate q value is chosen as the one corresponding to the minimum standard error and is estimated with an accuracy of at least 3 digits.

As is evident from these results, the mechanism of LRI drives the system's behavior away from BG statistics, only if the quartic potential is long range. Instead, when LRI apply only to the quadratic part, purely Gaussian pdfs are obtained.

In what follows, we will focus on the q values of the model under LRI with different exponents α_1, α_2. When these exponents are equal, as in Fig. 2(d), the value of q is practically unchanged. What we wish to examine now is how does q change when we apply LRI to the quartic potential and vary only the range of interactions in the quadratic part.

Thus, in the next section we proceed to examine which of the system's fundamental parameters affect the shape of the q–Gaussian pdfs and how the interaction range of the quadratic part of the potential affects the system's chaotic behavior.

4 Variation of q for different ranges and system parameters

As is well–known, q–Gaussian distributions are often associated with weak chaos and are linked to QSS which persist for very long times, until the system achieves energy equipartition at complete thermalization. In this regard, the precise value of q is significant, since it represents an entropic index. More specifically, the higher the value of q the more the solution remains at a QSS, as the orbits get trapped for long times in weakly chaotic regimes of phase space.

Our main purpose here is to investigate numerically the dependence of q on the system size N, the specific energy ε and the coupling constant b of the Hamiltonian (2). Let us mention at the outset that the parameters ε and b are not independent. Indeed, a simple rescaling of the Hamiltonian shows that the relevant parameter is $b\varepsilon$. Let us plot in Fig. 3 the dependence of q on ε for $N = 2048$ and $\alpha_1 \to \infty$. Note

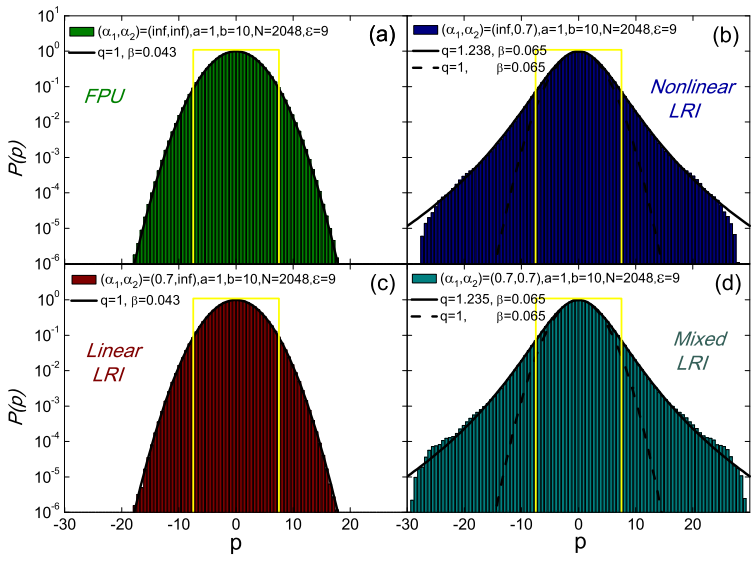

Figure 2: The momentum distributions for $N = 2048$ particles for the system (2). The upper panels show the cases: $\alpha_1 \to \infty$, $\alpha_2 \to \infty$, i.e. FPU (left) and $\alpha_1 \to \infty$, $\alpha_2 = 0.7$ (right). Lower panels show: $\alpha_1 = 0.7$, $\alpha_2 \to \infty$ (right) and $\alpha_1 = \alpha_2 = 0.7$ (right). The yellow lines correspond to the uniform distribution, from which the momenta where randomly extracted.

that the distribution becomes wider as ε increases (or b increases) nevertheless q tends to remain almost constant. In fact, Fig.3 clearly shows that q fluctuates around 1.23 and displays a greater tendency to converge as the specific energy increases.

When the linear LRI are switched on, the value of q, as shown in [11], is not affected and hence does not alter the statistical behavior of the system. As a consequence, the entropic parameter q turns out to be independent of the parameters ε, b and α_1.

On the other hand, when the system size increases, the value of q no longer remains a constant but also increases with N. From Fig. 4 it becomes evident that the corresponding q–Gaussian representing the statistics of the model spreads as N grows. Thus, choosing $\alpha_2 = 0.7$, $a = 1, b = 10$ and $\varepsilon = 9$ we find that the momentum histogram for low values of N is very close to a Gaussian, as shown in Fig. 4 for $N = 256$. It then deviates for $N = 512$ to a q–Gaussian with $q(N = 512) = 1.17$, which further increases

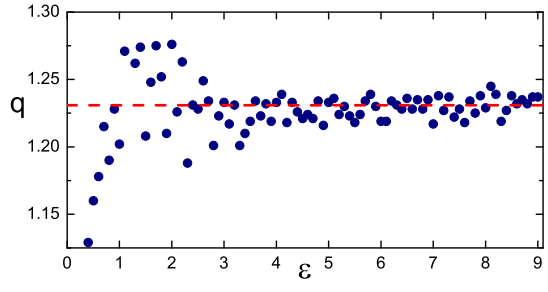

Figure 3: The dependence of q on ε, when LRI are applied to V_4 with $\alpha_2 = 0.7$, $\alpha_1 = \infty$, $a = 1$, $b = 10$ and $N = 2048$. The dashed line corresponds to a mean value of about $q = 1.23$.

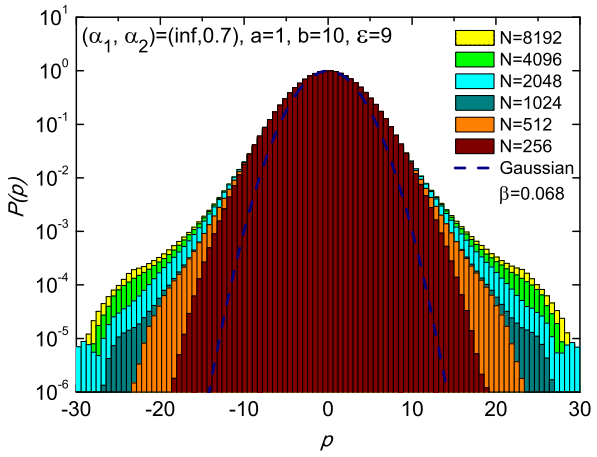

Figure 4: Momentum distributions for the system with $b = 10, \alpha_2 = 0.7$ and various N values. Note how the pdfs are described by a q–Gaussian of higher index q as N grows. More specifically, q ranges from 1.17 for $N = 512$ until 1.25 for $N = 8192$.

to $q(N = 1024) = 1.19$ and so on, as the weakly chaotic properties of the dynamics become more evident.

4.1 Asymptotic behavior of q in the limit $N \to \infty$

Extrapolating the value of q in the limit $N \to \infty$, we can now estimate the asymptotic value $q = q_\infty$ and also vary α_2 to determine the dependence of q_∞ on the interaction range applied to the quartic part of the potential at the thermodynamic limit. To this end, we consider a given value of $\alpha_2 < 1$ and systematically calculate the q dependence on N. In Fig. 5(a) we plot these q values versus $1/\log N$ and find that their dependence is accurately described by the following expression:

$$q(N, \alpha_2) = q_\infty(\alpha_2) - c(\alpha_2)/\log N \quad , \tag{4}$$

where $c(\alpha_2)$ is some constant. Each of the data in Fig. 5(a) has been plotted after performing 3 independent realizations of the momentum distributions and taking their average in the time window $[10^5, 5 \cdot 10^5]$.

This is important because it shows that the $q_\infty(\alpha_2)$ obtained from Fig. 5(a) by the intercept of the straight line Eq. (4) with the vertical axis (as $N \to \infty$) is larger than 1, which implies that the q–Gaussians are attractors in that limit. Next, plotting $q_\infty(\alpha_2)$ vs. α_2 in Fig. 5(b), we observe that it starts from 5/3 for $\alpha_2 = 0$, as predicted numerically and theoretically in [30], and then, after about $\alpha_2 = 0.2$, falls linearly towards 1. In particular, for $0.2 \leq \alpha_2 \leq 0.8$ the values of $q_\infty(\alpha_2)$ decrease as $q_\infty(\alpha_2) = 1.79 - 0.475\alpha_2$.

Note that the value of q reaches unity at $\alpha_2 = 1.5$ and not at the expected $\alpha_2 = 1$ threshold between short and long range interactions. This is a very interesting phenomenon and may be explained by the fact that q takes a very long time to converge to 1 over the range $1 \leq \alpha_2 \leq 1.4$.

5 Conclusions

In the present paper a generalization of the 1-dimensional Fermi-Pasta-Ulam β–model was studied, where two non–negative exponents α_1 and α_2 are introduced in the quadratic V_2 and quartic V_4 part of the potential to control the range of interactions. The role of long range interactions (LRI) on the system's

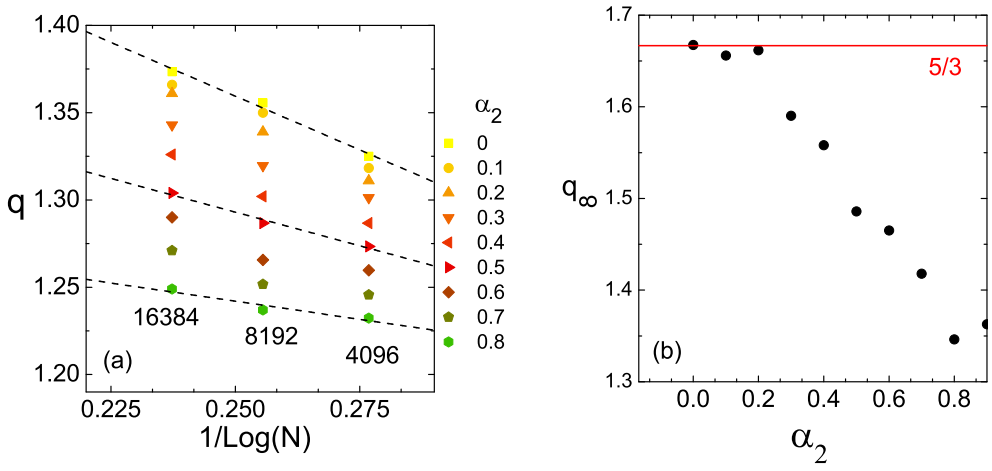

Figure 5: (a) The linear dependence of q on $1/\log N$ for $N = 4096, 8192, 16384$ depicted here provides an estimate for q_∞ in the thermodynamic limit, as α_2 changes. (b) The values of q_∞ are plotted here versus α_2. We have not included $\alpha_2 = 0.8$ in the above results due to the "noisy" behavior of q in the neighborhood $\alpha_2 = 1$. Nevertheless, for α_2 above 1.4, we definitively obtain $q = 1$. ($\varepsilon = 9$ in both panels.)

dynamical properties as well as its statistical behavior were examined in detail. In particular we concluded that only when LRI apply on V_4 and at high enough $b\varepsilon$ values: (a) the maximal Lyapunov exponent λ_{V4} decreases as a power-law with N (but eventually slows down and saturates to a positive value in the thermodynamic limit) and increases very slowly, as $\lambda_{V4} \sim \varepsilon^{0.05}$ ($b = 1$) with the specific energy, while at the same time (b) q–Gaussian pdfs of the momenta appear with $q > 1$. Both of these results indicate that LRI on V_4 is a necessary condition for what we call weak chaos in the FPU β–model, especially at high energies.

On the contrary, when LRI are applied to the *harmonic* part of the potential a much stronger type of chaos is encountered if the nonlinear interactions are short range. This is especially evident at low energies, indicating that the transition to large scale chaos occurs at much lower levels than in the classical FPU case. The corresponding MLE=λ_{V2} tends to saturate as a function of N, while, for small ε, λ_{V2} is much higher than the MLE=λ_{FPU} of the classical FPU model, with λ_{FPU} tending to λ_{V2} from below as $\varepsilon \to \infty$. All this is related to momentum pdfs of the purely Gaussian type ($q = 1$) and is associated with the strongest possible chaos and BG thermostatistics.

We also focused on the value of q in the momentum pdfs, when the main parameters of the problem vary. It turns out that q changes with N and α_2, while it remains unaltered if we increase the specific energy ε or widen the linear interactions, letting α_1 go closer to zero. In this direction, when $0 \leq \alpha_2 < 1$ we find a *linear* relation between q and $1/\log N$, which allows us to extrapolate the value of q to $q_\infty > 1$ at $N \to \infty$. This is important because it suggests that under these conditions BG thermostatistics no longer hold and q–Gaussian pdfs with $q > 1$ describe the true statistics in the thermodynamic limit.

Acknowledgments One of us (C.T.) gratefully acknowledges partial financial support by the Brazilian Agencies CNPq and Faperj, and by the John Templeton Foundation (USA). All of us acknowledge that this research has been co-financed by the European Union (European Social Fund–ESF) and Greek national funds through the Operational Program 'Education and Lifelong Learning' of the National Strategic Ref-

erence Framework (NSRF) - Research Funding Program: *Thales. Investing in knowledge society through the European Social Fund.*

References

[1] M. Antoni, S. Ruffo, *Phys. Rev. E* **52**, (1995) 2361-2374.

[2] V. Latora, A. Rapisarda, S. Ruffo, *Phys. Rev. Lett* **80**, (1998) 692.

[3] C. Anteneodo, C. Tsallis, *Phys. Rev. Lett.* **80**, (1998) 5313.

[4] T. Dauxois, V. Latora, A. Rapisarda, S. Ruffo, A. Torcini, Lecture Notes in Physics, edited by T. Dauxois, S. Ruffo, E. Arimondo, M. Wilkens, Vol. 602 (2002) p. 458.

[5] V.E. Tarasov, G.M. Zaslavsky, *Commun. Nonlinear Sci. Numer. Simul.* **11**, (2006) 885-898.

[6] K.A. Takeuchi, H. Chaté, F. Ginelli, A. Politi, A. Torcini, *Phys. Rev. Lett.* **107**, (2011) 124101.

[7] F. Ginelli, K.A. Takeuchi, H. Chaté, A. Politi, A. Torcini, *Phys. Rev. E* **84**, (2011) 066211.

[8] Th. Manos, S. Ruffo, *Trans. Theor. and Stat. Phys.* **40**, (2011) 360-381.

[9] D. Bagchi, C. Tsallis, *Sensitivity to initial conditions of d-dimensional long-range-interacting Fermi-Pasta-Ulam model: Universal scaling*, 1509.04697 [cond-mat.stat-mech].

[10] A. Ponno, H. Christodoulidi, *Asymptotic properties of the Fermi-Pasta-Ulam mean-field model in the thermodynamic limit*, preprint.

[11] H. Christodoulidi, C. Tsallis, T. Bountis, *EPL* **108**, (2014) 40006.

[12] H. Skokos, T. Bountis, Ch. Antonopoulos, Physica D **231**, (2007) 30-54.

[13] T. Bountis and H. Skokos, *Complex Hamiltonian Dynamics and Statistics*, Springer Series in Synergetics, Berlin (2012).

[14] M. Leo, R.A. Leo, P. Tempesta, *J. Stat. Mech.* (2010) P04021.

[15] M. Leo, R.A. Leo, P. Tempesta, C. Tsallis, *Phys. Rev. E* **85**, (2012) 031149.

[16] M. Leo, R.A. Leo, P. Tempesta, *Annals Phys.* **333**, (2013) 12-18.

[17] A. Pluchino, A. Rapisarda, C. Tsallis, *Europhys. Lett.* **80**, (2007) 26002.

[18] A. Pluchino, A. Rapisarda, C. Tsallis, *Europhys. Lett.* **83**, (2008) 30011.

[19] L.J.L. Cirto, Assis V., C. Tsallis, *Physica A* **393**, (2013) 286-296.

[20] S. Umarov, C. Tsallis, Steinberg S., *Milan J. Math.* **76**, (2008) 307-328.

[21] S. Umarov, C. Tsallis, M. Gell-Mann, S. Steinberg, *J. Math. Phys.* **51**, (2010) 033502.

[22] M.G. Hahn, X.X. Jiang, S. Umarov, *J. Phys. A* **43**, (16) (2010) 165208.

[23] H.J. Hilhorst, *J. Stat. Mech.* (2010) P10023.

[24] M. Jauregui, C. Tsallis, E.M.F. Curado, *J. Stat. Mech.* (2011) P10016.

[25] M. Jauregui, C. Tsallis, *Phys. Lett. A* **375**, (2011) 2085-2088.

[26] A. Plastino, M.C. Rocca, *Milan J. Math.* **80**, (2012) 243-249.

[27] C. Tsallis, A. Plastino, R.F. Alvarez-Estrada, *J. Math. Phys.* **50**, (2009) 043303.

[28] J.W. Gibbs, *Elementary Principles in Statistical Mechanics – Developed with Especial Reference to the Rational Foundation of Thermodynamics* (C. Scribner's Sons, New York, 1902; Yale University Press, New Haven, 1948; OX Bow Press, Woodbridge, Connecticut, 1981).

[29] Ch. Antonopoulos, T. Bountis, V. Basios, *Physica A* **390**, (2011) 3290-3307.

[30] C. Tsallis, *Introduction to Nonextensive Statistical Mechanics - Approaching a Complex World* (Springer, New York, 2009).

[31] C. Tsallis, *Stat. Phys.*, **52**, (1988) 479 [First appeared as preprint in 1987: CBPF-NF-062/87, ISSN 0029-3865, Centro Brasileiro de Pesquisas Fisicas, Rio de Janeiro].

[32] M. Gell-Mann, C. Tsallis, eds., *Nonextensive Entropy - Interdisciplinary Applications* (Oxford University Press, New York, 2004).

[33] C. Tsallis, Contemporary Physics **55**, (2014) 179-197.

[34] E. Fermi, J. Pasta, S. Ulam, Los Alamos, Report No. LA-1940, (1955). See also: Newell A.C., *Nonlinear Wave Motion*, Lectures in Applied Mathematics **15**, 143-155 (Amer. Math. Soc., Providence, 1974); Berman G.P. and Izrailev F.M., *Chaos* **15** (2005) 015104.

[35] G. Miloshevich, J.P. Nguenang, T. Dauxois, R. Khomeriki, S. Ruffo, *Phys. Rev. E* **91**, (2015) 032927.

[36] L. Casetti, R. Livi, and M. Pettini, *Phys. Rev. Lett.*, **74**, (1995) 375–378.